

Supporting Information

Solution-processed Self-powered Near-Infrared Photodetectors of Toxic Heavy Metal-Free AgAuSe Colloidal Quantum Dots

Zan Wang^{a, b, c, d}, Fenghua Liu^{b, c, d}, Yunjiao Gu^{b, c, d}, Yigu Hu^{b, c, d} and Weiping Wu*^{b, c, d}

^a. Institute of Photonics, Department of Optics and Optical Engineering, University of Science and Technology of China, Hefei, Anhui, 230026, China.

^b. State Key Laboratory of High Field Laser Physics, Chinese Academy of Sciences, Shanghai, 201800, China.

^c. Key Laboratory of Materials for High Power Laser, Chinese Academy of Sciences, Shanghai, 201800, China.

^d. Laboratory of Thin Film Optics, Shanghai Institute of Optics and Fine Mechanics, Chinese Academy of Sciences, Shanghai, 201800, China

Table of Contents

Figure S1. Low-magnification TEM images of Ag₂Se QDs.

Figure S2. The survey XPS spectra of Ag₂Se QDs and AgAuSe QDs.

Figure S3. (a) The photograph of the side products from the preparation of AgAuSe alloy QDs; TOF-SIMS analysis of the side products. (b–d) SIMS of the Ag⁺, Cl⁻, and AgClCl⁻ from the side products.

Figure S4. UV–Vis–NIR absorption spectrum of AgAuSe QDs films with different layers.

Figure S5. The 2D height profile AFM images of AgAuSe QDs films on, (a) 2-layer AgAuSe QDs film, (b) 3-layer AgAuSe QDs film; insert images are the curves of step height. (c) The thickness of the film varies with the number of layers

Figure S6. I-V characteristics of the Ag₂Se-EDT-based photodetector in dark and under an 808 nm NIR light with different illumination intensities.

Figure S7. The schematic diagram of the band alignment of the Au/AgAuSe QDs film/Au structure under illumination at a low bias voltage.

Figure S8. The dependences of absolute PLQY of the AgAuSe QDs with DT, EDT ligand and different states (colloid and film) emitted at 980 nm on various illumination intensities under 445 nm laser excitation.

Figure S9. Spectral responsivity and external quantum efficiency (EQE) of the photodetector under 0.05 mW/cm² light illumination and 0.5 V bias voltage.

Table S1. Comparison of the key parameters between the proposed photodetector and previous low dimension materials photodetectors.

The calculation formula of representative parameters.

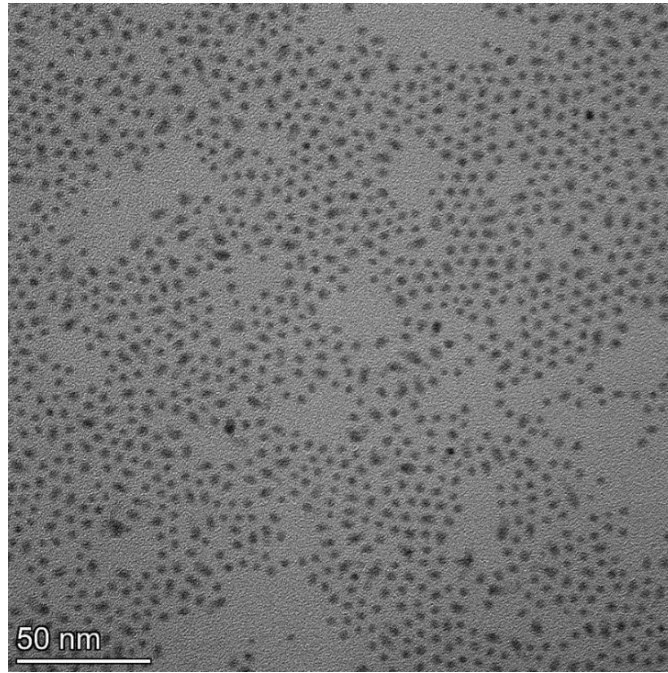


Figure S1. Low-magnification TEM images of Ag₂Se QDs.

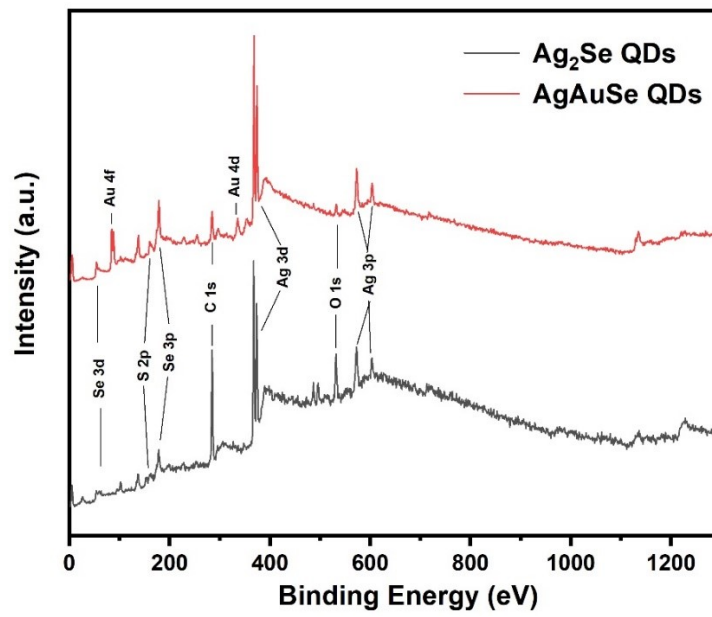


Figure S2. The survey XPS spectra of Ag₂Se QDs and AgAuSe QDs.

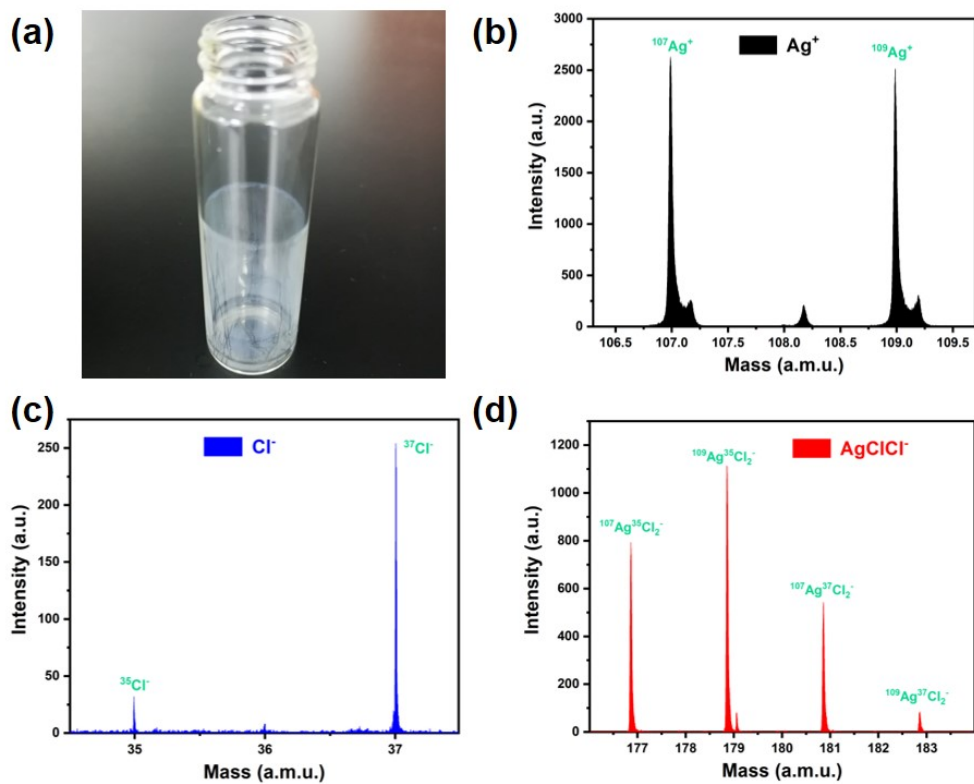


Figure S3. (a) The photograph of the side products from the preparation of AgAuSe alloy QDs; TOF-SIMS analysis of the side products. (b–d) SIMS of the Ag^+ , Cl^- , and AgClCl^- from the side products.

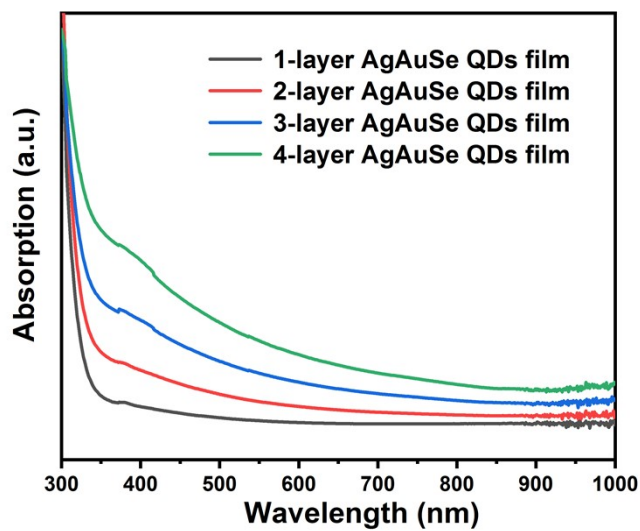


Figure S4. UV-Vis-NIR absorption spectrum of AgAuSe QDs films with different layers.

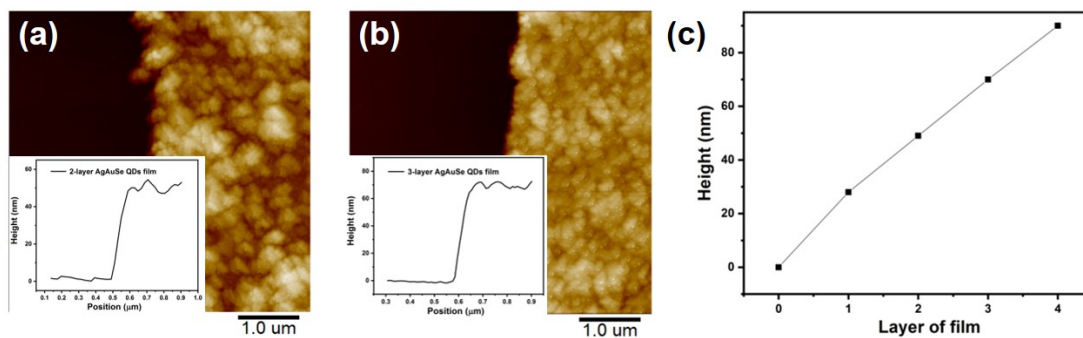


Figure S5. The 2D height profile AFM images of AgAuSe QDs films on, (a) 2-layer AgAuSe QDs film, (b) 3-layer AgAuSe QDs film; insert images are the curves of step height. (c) The thickness of the film varies with the number of layers.

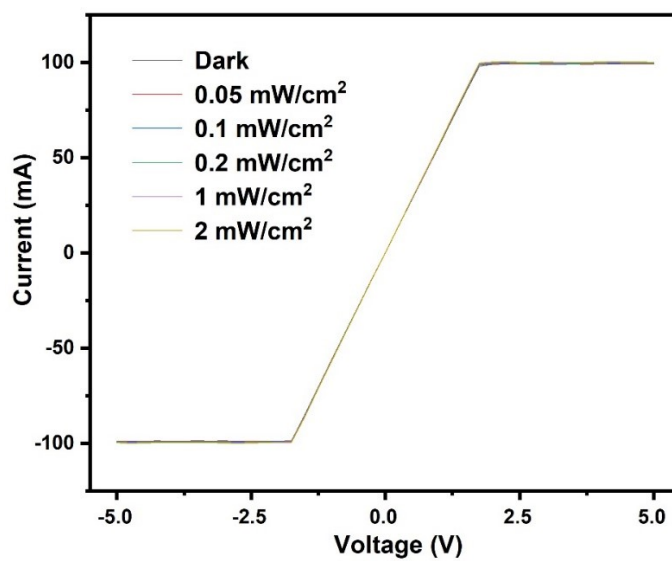


Figure S6. I-V characteristics of the Ag₂Se-EDT-based photodetector in dark and under an 808 nm NIR light with different illumination intensities.

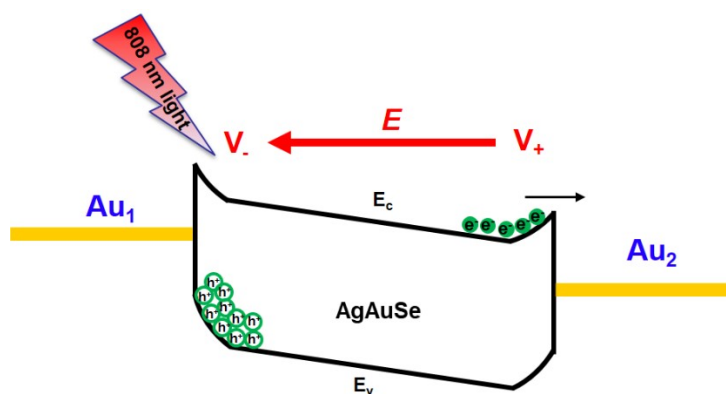


Figure S7. The schematic diagram of the band alignment of the Au/AgAuSe QDs film/Au structure under illumination at a low bias voltage.

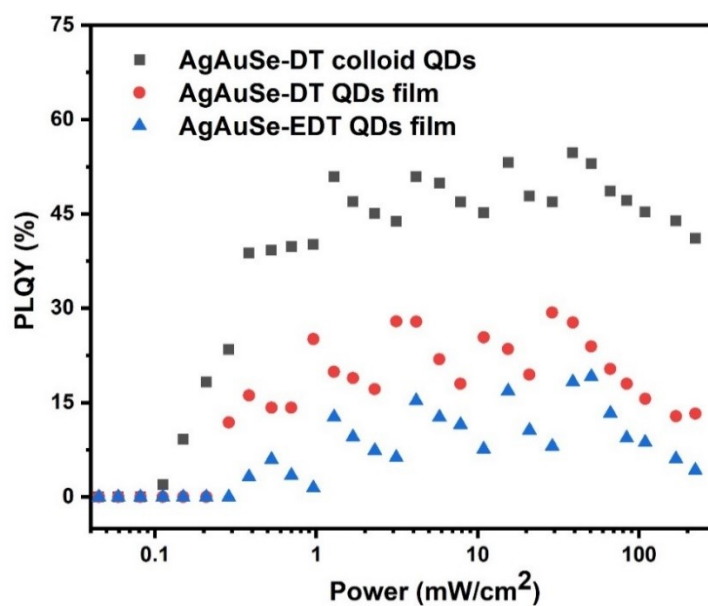


Figure S8. The dependences of absolute PLQY of the AgAuSe QDs with DT, EDT ligand and different states (colloid and film) emitted at 980 nm on various illumination intensities under 445 nm laser excitation.

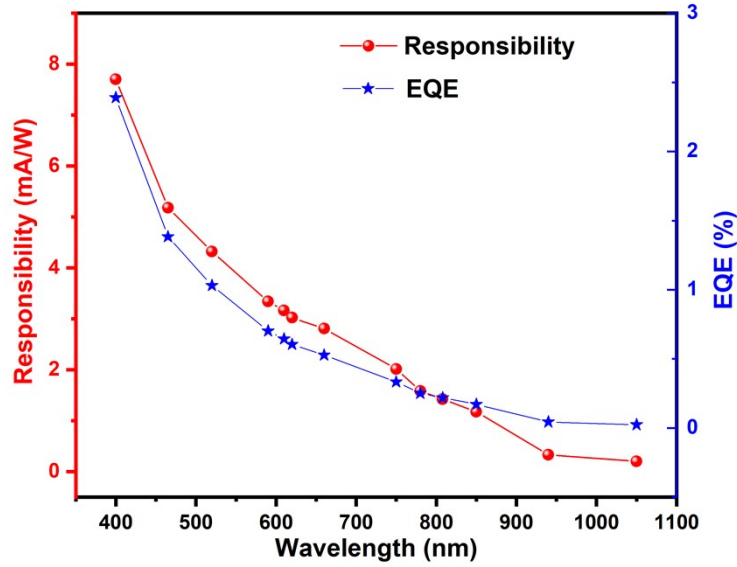


Figure S9. Spectral responsivity and external quantum efficiency (EQE) of the photodetector under 0.05 mW/cm² light illumination and 0.5 V bias voltage.

Table S1. Comparison of the key parameters between the proposed photodetector and previous low dimension materials photodetectors.

Devices	Self-powered	Bias [V]	Wavelength [nm]	R [mA/W]	D [Jones]	Ref.
Ag ₂ Se QDs	No	0.1-5	808	3	7.14×10 ⁹	1
PbS QDs/Ag NPs	No	40	850	3.8	1.5×10 ¹⁰	2
Ag ₂ Se QDs/ZnO	No	-4-2	2000	N/A	N/A	3
Ag ₂ Se QDs	No	2-4	2000-7000	0.5	N/A	4
Ag ₂ Se QDs/TiO ₂	No	-0.4-0.4	1200	4.17	N/A	5
CdSe/ZnS QDs	Yes	-2.5-2.5	532	0.003	2.43×10 ⁶	6
MoS ₂	No	10	1418	32	1×10 ⁹	7
CdSe QDs/PQT-12	Yes	-0.2-0.2	420	3.3	5.4×10 ⁹	8
AgAuSe QDs	Yes	-5-5	808	3.5	1.55×10 ¹⁰	This work

The three representative parameters (responsivity R , special detectivity D^* , external quantum efficiency EQE) were determined as follows:^{1,9}

$$R = \frac{I_{ph} - I_d}{P} \quad (S1)$$

$$D^* = \frac{A^{1/2} gR}{(2qg_d)^{1/2}} \quad (S2)$$

$$EQE = R \frac{hc}{q\lambda} \quad (S3)$$

Where I_{ph} is the photocurrent, I_d is the dark current, P is the radiated power (product of area and incident light density), A is the active area of the photodetector, q is the electron charge, h is Planck's constant, c is the speed of light, λ is the wavelength of incident light.

Reference:

- 1 W. Y. Lee, S. Ha, H. Lee, J. H. Bae, B. O. Jang, H. J. Kwon, Y. Yun, S. Lee and J. Jang, *Adv. Opt. Mater.*, 2019, **7**, 1900812.
- 2 J. G. He, K. K. Qiao, L. Gao, H. S. Song, L. Hu, S. L. Jiang, J. Zhong and J. Tang, *ACS Photonics*, 2014, **1**, 936–943.
- 3 M. Park, D. Choi, Y. Choi, H. B. Shin and K. S. Jeong, *ACS Photonics*, 2018, **5**, 1907–1911.
- 4 S. B. Hafiz, M. R. Scimeca, P. Zhao, I. J. Paredes, A. Sahu and D. K. Ko, *ACS Appl. Nano Mater.*, 2019, **2**, 1631–1636.
- 5 N. Graddage, J. Y. Ouyang, J. P. Lu, T. Y. Chu, Y. G. Zhang, Z. Li, X. H. Wu, P. R. L. Malenfant and Y. Tao, *ACS Appl. Nano Mater.*, 2020, **3**, 12209–12217.
- 6 L. F. Jin, Y. T. Zhang, Y. Yu, Z. L. Chen, Y. F. Li, M. X. Cao, Y. L. Che and J. Q. Yao, *Adv. Opt. Mater.*, 2018, **6**, 1800639.
- 7 Y. Xie, B. Zhang, S. X. Wang, D. Wang, A. Z. Wang, Z. Y. Wang, H. H. Yu, H. J. Zhang, Y. X. Chen, M. W. Zhao, B. B. Huang, L. M. Mei and J. Y. Wang, *Adv. Mater.*, 2017, **29**, 1605972.
- 8 H. Kumar, Y. Kumar, G. Rawat, C. Kumar, B. Mukherjee, B. N. Pal and S. Jit, *IEEE Photonics Technol. Lett.*, 2017, **29**, 1715–1718.
- 9 R. Saran and R. J. Curry, *Nat. Photonics*, 2016, **10**, 81–92.